Monograph:
Edwards, J.B. and Guilandoust, M (1980) An Analytically-Derived, Parametric Transfer-Function Model for Ideal, Packed, Binary Distillation Columns. Research Report. ACSE Report 139 . Department of Control Engineering, University of Sheffield, Mappin Street, Sheffield

AN ANALYTICALLY-DERIVED, PARAMETRIC TRANSFER-FUNCTION MODEL FOR IDEAL, PACKED, BINARY DISTILLATION COLUMNS

PART I MODEL DEVELOPMENT

by

J.B. Edwards, B.Sc.(Eng.), M.Sc., C.Eng., M.I.E.E.

and M. Guilandoust*, B.Sc., M.Sc.

Senior Lecturer, Dept. of Control Engineering,
University of Sheffield,
Mappin Street, Sheffield S1 3JD.

Research Report No. 139

July 1980

AN ANALYTICALLY-DERIVED, PARAMETRIC TRANSFER-FUNCTION MODEL FOR IDEAL PACKED, BINARY DISTILLATION COLUMNS

PART I

Summary

Partial differential equations and boundary conditions are derived for the large- and small-signal behaviour of compositions in an ideal, symmetrical spatially-continuous (packed) distillation column separating a binary mixture. A precise parametric transfer-function matrix (T.F.M.) for the system is derived completely analytically so allowing the calculation of the parameters of the T.F.M. directly from those of the plant.

It is shown that the correct choice of input and output vectors yields a completely diagonal system (i.e. the system is Dyadic in structure).

The investigation reveals important differences between the behaviour of packed and tray-type distillation columns examined in companion papers. In particular, important non-minimum phase effects are shown to occur in some packed columns that are not found in tray types.

AN ANALYTICALLY-DERIVED, PARAMETRIC TRANSFER-FUNCTION MODEL FOR IDEAL PACKED, BINARY DISTILLATION COLUMNS

PART I

Introduction

An obviously desirable though not easily attainable objective in any process modelling exercise is to obtain a parametric transfer-function matrix (T.F.M.) governing the small signal behaviour of the particular process in question. Such a model has two important assets:

(a) it is immediately usable in modern techniques for multi-variable control systems design (which are based in the frequency domain),

and (b) being a parametric model, the effects on control of changes to the constructional and operational parameters of the plant can be immediately assessed without the need for reidentification.

The calculation of parametric T.F.M. models however requires the derivation and analytical solution of the linearised process equations for sinusoidal inputs. The broad class of counterflow processes to which distillation belongs involves spatially distributed heat and mass transfer, (and sometimes chemical change), so that the process equations are either differential equations of very high order or partial differential equations (p.d.e's). Furthermore, and perhaps more importantly, such processes are of a multistage type with difficult boundary conditions pertaining at the interfaces between stages. Chiefly for this reason, whilst analytical dynamic solutions have been derived for the simpler single-stage processes (e.g., liquid/liquid heat exchangers and solvent extractors), processes of two or more stages such as distillation columns (and the more difficult single-stage processes) have defied attempts at complete solution. Despite vigorous investigations of distillation over more than 20 years, resort has ultimately been made to part-empirical solutions[1,2], black-box testing or one-off simulation yielding results satisfactory to only one column under one set of operating conditions. This challenge has therefore provided one important motivation for the research here reported in which a T.F.M. model is derived for the normal 2-stage binary column by completely analytical means so that the T.F.M. parameters are directly related to adjustable plant parameters. The only approximations involved are those normally associated

with linearisation. Symmetrical construction and operation, which generally implies good plant design, have been assumed.

An equally important inspiration has been the research of Owens[3] on multivariable process model approximations used as a basis for control system design. His control design rules for multivariable first-order lag processes, requiring knowledge of only the high-and low-frequency gain matrix, have already been successfully applied jointly by Owens and the present author (J.B.E) to simulated heat exchangers and columns. In establishing the limits of applicability of the completely analysable heat exchangers nowever it was discovered that lobes in the true system frequency response, resulting from travelling waves in the process, cause some deviation from the first-order lag model behaviour and, under high controller gain, oscillation or instability could result. A multivariable structure involving lags and delays is therefore necessary to represent the process more precisely so leading to the concept of a multivariable lag-delay model for more general application. Before formulating so general a structure and for rigorous testing of such a model later, it has therefore been necessary to examine a much more complex counter-flow process. The binary distillation column has here been chosen with these objectives in mind.

The present paper is devoted to packed distillation columns and is concerned with the analytical derivation of the parametric transfer-function matrix model. A second paper[5] deals with the interpretation of the model for predicting system behaviour. A third and fourth paper (in this companion set of four) provide a similar treatment of tray-type distillation columns. Important differences in the behaviour of the two types of column are revealed .

The columns are idealised in terms of the mixture separated, adiabatic operation, their symmetrical construction, operation and feed conditions and through the neglect of all dynamics other than those directly associated with composition change. Model elaboration may be undertaken in later research but, in what the authors, believe to be the first ever accurate, analytical solution for composition change, these idealisations have proved to be essential aids to model development and model interpretation. It is believed that the model and its derivation expose the primary, underlying driving forces of column dynamics.

1. Large signal model

The process is illustrated diagrammatically in Fig. 1 which shows the various liquid and vapour flow rates through the system. It will be noted

that height h' is defined from an origin at the feed point for preliminary analyses. Fig. 2 shows the cross flow taking place from the liquid to vapour streams within a thin conceptual cell of thickness $\delta h'$ at a height $h' = n\delta h'$.

1.1 Vapour/liquid equilibrium

If Y,X are the compositions† of the vapour and liquid in the rectifier respecitvely and Y', X' those in the stripper, then the equilibrium vapour compositions Y_e,(Y_e'), for a given liquid composition X, (X') are governed by

$$\beta = Y_e(1-X)/\{X(1-Y_e)\} \text{ and } \beta = Y_e'(1-X')/\{X'(1-Y_e')\} \quad (1)$$

where β is the "Relative Volatility" which is constant for an ideal mixture (i.e. one obeying Dalton's and Rayoult's laws). The equilibrium relationship, (1), takes the form shown in Fig. 3 in which straight-line approximations for the stripper and rectifier are also shown. The symmetry of both the true equilibrium curve and its piecewise linear approximation about the -45° line is noteworthy.

For symmetry the equations of the straight-line segments are

$$Y_e' = \alpha X' \quad \text{, for the stripper} \quad (2)$$

and

$$Y_e = X/\alpha + (\alpha-1)/\alpha \quad \text{, for the rectifier} \quad (3)$$

where

$$\beta > \alpha = 1 + \varepsilon \quad \text{, } \varepsilon > 0 \quad (4)$$

1.2 Large-signal partial differential equations

Considering the nth rectifier cell shown in Fig. 2, material balances on the vapour and liquid streams for the light component give

$$\begin{aligned} H_v\,\delta h'\,\frac{d}{dt}Y(n) &= V_r\{Y(n-1)-Y(n)\} + k_r\{Y_e(n) - Y(n)\}\delta h' \\ H_\ell\,\delta h'\,\frac{d}{dt}X(n) &= L_r\{X(n+1) - X(n)\} - k_r\{Y_e(n) - Y(n)\}\delta h' \end{aligned} \quad (5)$$

where H_v and H_ℓ are the vapour and liquid capacitances p.u. length and k_r is a constant coefficient of cross flow. As $\delta h'$ is made infinitesimal we therefore obtain the following p.d.e.'s governing the truly spatially continuous process (using eqn(3) for the second p.d.e.)

$$\left.\begin{aligned} H_v\partial X/\partial t + V_r\partial Y/\partial h' &= k_r(Y_e - Y) \\ -H_\ell\alpha\partial Y_e/\partial t + L_r\alpha\partial Y_e/\partial h' &= k_r(Y_e - Y) \end{aligned}\right\} \quad (6)$$

Similarly, for the stripper (h' < O) we obtain

† Compositions expressed as mole fractions of the lighter component in the binary mixture.

$$\left.\begin{aligned} -H_\ell'\,\partial X'/\partial t + L_s\,\partial X'/\partial h' &= k_2(X' - X_e') \\ H_v'\alpha\partial X_e'/\partial t + \alpha V_s\,\partial X_e'/\partial h' &= k_s\,(X' - X_e') \end{aligned}\right\} \quad (7)$$

where H_ℓ', H_v' are again liquid and vapour capacitances p.u. length and k_s the cross-flow coefficient for the stripper and

$$X_e' \triangleq Y'/\alpha \quad (8)$$

1.3 Preliminary conditions for symmetry

If the system is built and run such that nominally

$$V_r = \alpha L_r \quad , \quad L_s = \alpha V_s \quad (9)$$

$$k_s = k_r = k \quad (10)$$

$$L_s = V_r = V \quad (11)$$

$$\left.\begin{aligned} H_v &= H_v'\alpha = H_1 \\ H_\ell' &= H_\ell\alpha = H_2 \end{aligned}\right\} \quad (12)$$

then clearly the system becomes highly symmetrical, p.d.e.'s (6) and (7) reducing to

$$\left.\begin{aligned} H_1\,\partial Y/\partial t + V\,\partial Y/\partial h' &= k(Y_e - Y) \\ -H_2\,\partial Y_e/\partial t + V\partial Y_e/\partial h' &= k(Y_e - Y) \\ -H_2\,\partial X'/\partial t + V\partial X'/\partial h' &= k(X' - X_e') \\ H_1\partial X_e'/\partial t + V\partial X_e'/\partial h' &= k(X' - X_e') \end{aligned}\right\} \quad (13)$$

1.4 P.d.e.'s in normalised space and time

Expressing normalised distance as

$$h = h'k/V \quad (14)$$

and normalised time as

$$\tau = t\,k/H_2 \quad (15)$$

then the p.d.e.'s (13), for the symmetrical system, reduce to the simplified form

$$\left.\begin{aligned} c\,\partial Y/\partial\tau + \partial Y/\partial h &= Y_e - Y \\ -\partial Y_e/\partial\tau + \partial Y_e/\partial h &= Y_e - Y \\ -\partial X'/\partial\tau + \partial X'/\partial h &= X' - X_e' \\ c\partial X_e'/\partial\tau + \partial X_e'/\partial h &= X' - X_e' \end{aligned}\right\} \quad (16)$$

where $$c = H_1/H_2 \quad (17)$$

1.5 Feed-point boundary conditions

Considering a thin cell at the feed point then it is clear that as its

thickness $\delta h' \to 0$ so the cross-flow from liquid to vapour and the accumulation terms vanish as the area for transfer and the cell volume $\to 0$. We are therefore left with, in general

$$\left.\begin{aligned} V_s\, Y'(0) + F_v\, z &= V_r\, Y(0) \\ \text{and} \qquad L_r\, X(0) + F_\ell Z &= L_s\, X'(0) \end{aligned}\right\} \qquad (18)$$

where z and Z are the compositions of the feed vapour and liquid (see Fig. 1).

1.6 Terminal boundary conditions

1.6.1 Accumulator

At the top of the rectifier, as shown in Fig. 1, liquid is simply condensed from vapour at composition $Y(L_1)$, where L_1 is the normalised rectifier height and returned at flow rate L_r to the column. Hence the top boundary condition is

$$H_a \frac{dX}{dt}(L_1) = V_r\, Y(L_1) - (L_r + D)X(L_1)$$

where H_a is the constant capacitance of the accumulator and D the distillate rate. For a constant volume within the accumulator however, as Fig. 1 shows,

$$V_r = L_r + D \qquad (19)$$

so that

$$H_a \frac{dX}{dt}(L_1) = V_r\{Y(L_1) - X(L_1)\} \qquad (20)$$

and using (3) to eliminate $X(L_1)$ in terms of $Y_e(L_1)$ we obtain

$$H_a \alpha \frac{dY_e}{dt}(L_1) = V_r\left[\alpha\{1-Y_e)L_1)\}-\{1-Y(L_1)\}\right] \qquad (21)$$

1.6.2 Reboiler

In the reboiler, at normalised distance L_2 below the feed point, (i.e. at $h = -L_2$), we have, if the reboiler liquid is in equilibrium with its vapour,

$$H_b \frac{dX'_e}{dt}(-L_2) = L_s X'(-L_2) - (V_s + W)Y'(-L_2)$$

but

$$L_s = V_s + W \qquad (22)$$

so that, eliminating $Y'(-L_2)$ using equation (8), we obtain the lower boundary condition in the form:

$$H_b \frac{dX'_e}{dt}(-L_2) = L_s\, X'(-L_2) - \alpha X'_e(-L_2) \qquad (23)$$

where H_b is the fixed capacitance of the reboiler.

Clearly there exists a strong symmetry between the accumulator and reboiler boundary conditions (21) and (23), if L is set equal to V as specified by (11).

1.7 Steady-state solution of the symmetrical system

1.7.1 Feed conditions for symmetry

It follows implicitly from overall mass balance considerations and special case equations (9) and (11) that

$$F_v = F_\ell \triangleq F \qquad \ldots(24)$$

and from (24) in conjunction with equations (4), (9), (11), (19) and (21) it follows also that the column must be run such that nominally

$$D = W = F = \varepsilon L_r \qquad \ldots(25)$$

If the feed compositions are also specified such that

$$z = 1-Z \qquad \ldots(26)$$

i.e. the feed coordinates lie on the -45° line in Fig.3 and if the feed mixture is in equilibrium such that

$$z = \alpha Z \qquad \ldots(27)$$

from which we deduce

$$Z = 1/(1+\alpha) \qquad \ldots(28)$$

then the feed boundary conditions also become highly symmetric to one another since they may now be expressed thus:

$$X_e'(0) + \{1-Y(0)\} = 2/(\alpha+1) \qquad \ldots(29)$$

and

$$\{1-Y_e'(0)\} + X'(0) = 2/(\alpha+1) \qquad \ldots(30)$$

1.7.2 Steady-state solutions

Ignoring all time-derivatives, steady-state solutions for the normalised system p.d.e.'s (16) may be obtained subject to the special case boundary conditions (21), (23), (29) and (30) as shown in appendix 1, producing the following results:

$$\frac{\partial Y}{\partial h} = \frac{\partial Y_e}{\partial h} = \frac{\partial X'}{\partial h} = \frac{\partial X_e'}{\partial h} = G = \text{constant} \qquad \ldots(31)$$

where

$$G = 2\varepsilon/\{(\alpha+1)(2\varepsilon L+\alpha+1)\} \qquad \ldots(32)$$

provided

$$L_1 = L_2 = L \qquad \ldots(33)$$

(i.e. provided rectifier and stripper are of equal length).

$$\left.\begin{aligned} \text{Hence} \quad Y(h) &= Y(0) + Gh \\ Y_e(h) &= Y_e(0) + Gh \end{aligned}\right\} \quad \ldots(34)$$

$$\left.\begin{aligned} \text{where} \quad Y(0) &= 1 - 2(\alpha+\varepsilon L)/\{(\alpha+1)(2\varepsilon L+\alpha+1)\} \\ \text{and} \quad Y_e(0) &= 1 - 2(1+\varepsilon L)/\{(\alpha+1)(2\varepsilon L+\alpha+1)\} \end{aligned}\right\} \quad \ldots(35)$$

Furthermore it is shown in appendix 1 that the following symmetry exists between the compositions in the stripper and rectifier, viz,

$$\left.\begin{aligned} X'(-h) &= 1 - Y(h) \\ X_e'(-h) &= 1 - Y_e(h) \end{aligned}\right\} \quad \ldots(36)$$

The steady-state composition profiles are therefore linear in h and are shown geometrically in Fig.4.

The steady-state large-signal equations and their solutions stated above are essential to the parametric modelling of the small signal behaviour of the system which is considered in the next section of this report.

2. Small signal model

The small signal p.d.e.'s for the system may be derived by implicit differentiation of the general large signal p.d.e.'s (6) and (7). Denoting small perturbations by lower-case letters we therefore obtain

$$\left.\begin{aligned} &H_v \partial y/\partial t + V_r \partial y/\partial h' + (\partial Y/\partial h')v = k_r(y_e - y) \\ &-H_\ell \alpha \partial y_e/\partial t + L_r \alpha \partial y_e/\partial h' + (\partial Y_e/\partial h')\alpha\ell = k_r(y_e - y) \end{aligned}\right\} \quad \ldots(37)$$

$$\left.\begin{aligned} &-H_\ell' \partial x'/\partial t + L_s \partial x'/\partial h' + (\partial X'/\partial h')\ell = k_s(x' - x_e') \\ &H_v' \alpha \partial x_e'/\partial t + V_s \alpha \partial x_e'/\partial h' + (\partial X_e'/\partial h')\alpha v = k_s(x' - x_e') \end{aligned}\right\} \quad \ldots(38)$$

Regarding the upper-case symbols as quasi-constants and inserting the conditions for symmetrical steady-state solutions produces the simplified system:

$$
\left.
\begin{aligned}
H_1 \partial y/\partial t + V\partial y/\partial h' + kGv/V &= k(y_e - y) \\
-H_2 \partial y_e/\partial t + V\partial y_e/\partial h' + kG\,\ell/V &= k(y_e - y) \\
-H_2 \partial x'/\partial t + V\partial x'/\partial h' + kG\ell/V &= k(x' - x_e') \\
H_1 \partial x_e/\partial t + V\partial x_e'/\partial h' + kG\alpha v/V &= k(x' - x_e')
\end{aligned}
\right\} \quad \ldots(39)
$$

recalling that $\partial/\partial h' \equiv (k\partial/\partial h)/V$ ...(40)

2.1 Normalising small signal p.d.e.'s

Expressing the perturbation derivatives now with respect to normalised distance h (=h'k/V) and time τ (=tk/H_2) in a manner similar to the large signal p.d.e.'s (16) the system further simplifies to

$$
\left.
\begin{aligned}
c\,\partial y/\partial \tau + \partial y/\partial h + Gv/V &= y_e - y \\
-\partial y_e/\partial \tau + \partial y_e/\partial h + \alpha G\ell/V &= y_e - y \\
-\partial x'/\partial \tau + \partial x'/\partial h + G\ell/V &= x' - x_e' \\
c\,\partial x_e'/\partial \tau + \partial x_e'/\partial h + \alpha Gv/V &= x' - x_e'
\end{aligned}
\right\} \quad \ldots(41)
$$

recalling that $c = H_1/H_2$.

2.2 Inverted U-tube model

As will be demonstrated, solution for the terminal perturbations (i.e. perturbations at the accumulator and reboiler ends of a two stage process such as the column under investigation) is greatly simplified by conceptually bending the process into the form of an inverted U-tube as shown in Fig.5 redefining the origin of h and h' now at the reboiler end as shown rather than at the feed plate. This clearly has the effect of reversing the sign of the spatial derivatives in the rectifier so that, in terms of our newly defined h, equations (41) become modified to

$$
\left.
\begin{aligned}
c\,\partial y/\partial \tau - \partial y/\partial h + Gv/V &= y_e - y \\
-\partial y_e/\partial \tau - \partial y_e/\partial h + \alpha G\ell/V &= y_e - y \\
-\partial x'/\partial \tau + \partial x'/\partial h + G\ell/V &= x' - x_e' \\
c\,\partial x_e'/\partial \tau + \partial x_e'/\partial h + \alpha Gv/V &= x' - x_e'
\end{aligned}
\right\} \quad \ldots(42)
$$

Ignoring initial conditions and taking Laplace transforms of (42) in p with respect to τ and in s with respect to h gives

$$\left.\begin{aligned}
(1+cp-s)\tilde{\tilde{y}} - \tilde{\tilde{y}}_e + G\tilde{v}/Vs + \tilde{y}(0) &= 0 \\
-(1+p+s)\tilde{\tilde{y}}_e + \tilde{\tilde{y}} + G\tilde{\ell}/Vs + \tilde{y}_e(0) &= 0 \\
-(1+p-s)\tilde{\tilde{x}}' + \tilde{\tilde{x}}_e' + G\tilde{\ell}/Vs - \tilde{x}'(0) &= 0 \\
(1+cp+s)\tilde{\tilde{x}}_e' - \tilde{\tilde{x}}' + \alpha G\tilde{v}/Vs - \tilde{x}_e'(0) &= 0
\end{aligned}\right\} \quad \ldots(43)$$

Where superscript $\tilde{}$ denotes transforms w.r.t. h and τ and $\tilde{}$ w.r.t. τ only.

It is important also to note that $\tilde{y}(0)$ etc now refers to variables at the ends of the column not at the feed point.

In the present study attention is to be confined to columns which are not only spatially, but also dynamically symmetrical. This demands the equality of the vapour and liquid capacitances H_1 and H_2 so that, in this special case

$$c = 1 \qquad \ldots(44)$$

implying high pressure distillation.

2.3 Matrix representation

Great advantage may now be taken of the system symmetry permitting the very simple matrix representation of the system which in conjunction with the inverted U-tube concept, leads rapidly to solutions for the terminal composition variations. Being so straightforward, the solutions yield considerable insight into the underlying cause/effect relationships which drive the column behaviour.

In particular, if input and output vectors are defined thus

$$\underline{q} = \begin{pmatrix} y-x' \\ y+x' \end{pmatrix}, \quad \underline{r} = \begin{pmatrix} y_e-x_e' \\ y_e+x_e' \end{pmatrix} \quad \text{and} \quad \underline{u} = \frac{G}{V}\begin{pmatrix} v+\ell \\ v-\ell \end{pmatrix} \qquad \ldots(45)$$

then, if c = 1, adding and subtracting analogous pairs of equations in set (43) clearly produces the simple system

$$(1+p-s)\,\underset{\sim}{\underset{\sim}{q}} - \underset{\sim}{\underset{\sim}{r}} = -s^{-1}\underset{\sim}{u} - \underset{\sim}{q}(0) \qquad \ldots(46)$$

$$-(1+p+s)\,\underset{\sim}{\underset{\sim}{r}} + \underset{\sim}{\underset{\sim}{q}} = \alpha s^{-1}\begin{pmatrix} -1 & \\ & 1 \end{pmatrix}\underset{\sim}{u} - \underset{\sim}{r}(0) \qquad \ldots(47)$$

2.3.1 Terminal boundary conditions

For small perturbations these are obtained by implicit differentiation of the general large signal boundary conditions (21) and (23), giving in terms of the newly defined height origin,

$$H_a\,\alpha\,dy_e(0)/dt = V_r\{y(0) - \alpha y_e(0)\}$$

and $$H_b\,dx_e'(0)/dt = L_s\{x'(0) - \alpha x_e'(0)\}$$

. Recalling that normalised time $\tau = tk/H_2$ and that nominally $V_r = L_s = V$ for symmetry then

$$\frac{H_a\,\alpha\,k}{H_2\,V}\,\frac{dy_e(0)}{d\tau} = y(0) - \alpha y_e(0)$$

and

$$\frac{H_b\,k}{H_2\,V}\,\frac{dx_e'(0)}{d\tau} = x'(0) - \alpha x_e'(0)$$

so that, in terms of Laplace transforms in p, we have

$$\tilde{y}_e(0) = \alpha^{-1}h_a(p)\,\tilde{y}(0)$$

and $$\tilde{x}_e'(0) = \alpha^{-1}h_b(p)\,\tilde{x}'(0) \qquad \ldots(48)$$

where the accumulator and reboiler transfer-function $h_a(p)$ and $h_b(p)$ are given by

$$h_a(p) = 1/(1+T_a p)$$

$$h_b(p) = 1/(1+T_b p) \qquad \ldots(49)$$

where $$T_a = H_a k/(H_2 V)$$

and $$T_b = H_b k/(H_2 V\alpha) \qquad \ldots(50)$$

If again we assume symmetry such that

$$h_a(p) = h_b(p) \triangleq h_e(p) \qquad \ldots(51)$$

then from (45) and (48) it is clear that the terminal boundary conditions may be expressed in the compact matrix form

$$\tilde{\underline{r}}(0) = \alpha^{-1} h_e(p) \tilde{\underline{q}}(0) \qquad \ldots(52)$$

so permitting the elimination of, say, $\tilde{\underline{r}}(0)$ from (46) and (47). Doing this and then obtaining separate expressions for $\tilde{\underline{q}}$ and $\tilde{\underline{r}}$ yields

$$\tilde{\underline{q}} = (s^2-q^2)^{-1}\{(1+p-h_e\alpha^{-1}+s)\tilde{\underline{q}}(0)+s^{-1}\begin{bmatrix} 1+p-\alpha+s & \\ & 1+p+\alpha+s \end{bmatrix}\tilde{\underline{u}}\} \qquad \ldots(53)$$

and

$$\tilde{\underline{r}} = (s^2-q^2)^{-1}\{[1-h_e\alpha^{-1}(1+p)+h_e\alpha^{-1}s]\tilde{\underline{q}}(0)+s^{-1}\begin{bmatrix} 1-(1+p)\alpha+\alpha s & \\ & 1+(1+p)\alpha-\alpha s \end{bmatrix}\tilde{\underline{u}}\} \qquad \ldots(54)$$

where q is an important irrational function of Laplace variable p, being given by

$$q^2 = p^2 + 2p \qquad \ldots(55)$$

Inverting equations (53) and (54) back to the h,p domain from the s,p domain, with the aid of Laplace-transform tables, gives

$$\tilde{\underline{q}}(h) = \{\left(\frac{1+p-h_e\alpha^{-1}}{q}\right)\sinh q\,h + \cosh q\,h\}\tilde{\underline{q}}(0)$$

$$+\begin{bmatrix} \frac{(1+p-\alpha)}{q^2}(\cosh qh-1) + \frac{\sinh qh}{q} & \\ & \frac{(1+p+\alpha)}{q^2}(\cosh qh-1) + \frac{\sinh qh}{q} \end{bmatrix}\tilde{\underline{u}} \qquad \ldots(56)$$

and

$$\tilde{\underline{r}}(h) = \{\frac{[1-h_e\alpha^{-1}(1+p)]}{q}\sinh qh + h_e\alpha^{-1}\cosh qh\}\tilde{\underline{q}}(0)$$

$$+\begin{bmatrix} \frac{\{1-(1+p)\alpha\}}{q^2}(\cosh qh-1) + \frac{\alpha\sinh qh}{q} & \\ & \frac{\{1+(1+p)\alpha\}}{q^2}(\cosh qh-1) - \frac{\alpha\sinh qh}{q} \end{bmatrix}\tilde{\underline{u}} \qquad \ldots(57)$$

Now $\tilde{q}(0)$ is the vector of combinations of terminal compositions and is therefore the output vector of prime interest in an investigation of column performance since it relates to column outputs in the process engineering sense of the word. It can clearly be calculated by setting h = L (i.e. the new feed point coordinate) in (56) and (57) and substituting known boundary condition relationships between $\tilde{q}(L)$ and $\tilde{r}(L)$. These boundary conditions are therefore derived and substituted in the following section of the report.

2.3.2 Feed boundary conditions

• Implicit differentiation of the general large-signal boundary conditions (18) for constant feed flows and compositions yields

$$V_s\, y'(0) - V_r\, y(0) + \{Y'(0) - Y(0)\}v = 0$$

and

$$L_r\, x(0) - L_s\, x'(0) + \{X(0) - X'(0)\}\ell = 0$$

Replacing x(0) and y'(0) by $\alpha y_e(0)$ and $\alpha x_e'(0)$ {see equations (3) and (8)} and substituting the steady-state flow conditions for symmetry {equations (9) and (11)} gives

$$x_e'(0) - y(0) - \{Y(0) - Y'(0)\}v/V = 0$$

$$y_e(0) - x'(0) + \{X(0) - X'(0)\}\ell/V = 0$$

and using steady-state solutions (31) to (36) for Y(0) etc finally produces

$$y(0) = x_e'(0) - (\varepsilon/2)Gv/V$$

$$x'(0) = y_e(0) + (\varepsilon/2)G\ell/V$$

Now these equations are written in notation pertaining to the straight column model rather than the inverted U-tube model for which we must substitute h = L for h = 0 so transforming the above equations to read

$$\left.\begin{aligned} y(L) &= x_e'(L) - (\varepsilon/2)Gv/V \\ x'(L) &= y_e(L) + (\varepsilon/2)G\ell/V \end{aligned}\right\} \quad \ldots(58)$$

Adding and subtracting equations (58) clearly produces the compact matrix equation

$$\underline{q}(L) = \begin{pmatrix} -1 & \\ & 1 \end{pmatrix} \underline{r}(L) - (\tfrac{\varepsilon}{2})\, \underline{u} \qquad (59)$$

which is readily substituted into general solutions (56) and (57) to permit calculation of $\underline{q}(0)$.

2.4 Calculation of output composition vectors

Substituting h = L in matrix equations (56), (57) and, using (59), the terms of output vector $\tilde{\underline{q}}(0)$ are now calculated individually.

For $\tilde{q}_1(0)$ we note from (59) that

$$\tilde{q}_1(L) + \tilde{r}_1(L) + (\varepsilon/2)\tilde{u}_1 = 0$$

so that, recalling that $q^2 = p(2+p)$

$$\tilde{q}_1(0,p) = \frac{\{(\alpha-1)(\cosh qL-1)p^{-1} - (1+\alpha)(\sinh qL)q^{-1} - \varepsilon/2\}}{\{(1-h_e\alpha^{-1})(\sinh qL)qp^{-1} + (1+h_e\alpha^{-1})\cosh qL\}}\ \tilde{u}_1(p) \qquad (60)$$

for $\tilde{q}_2(0)$ we note from (59) that

$$\tilde{q}_2(L) - \tilde{r}_2(L) + (\varepsilon/2)\tilde{u}_2 = 0$$

so that

$$\tilde{q}_2(0,p) = \frac{\{(\alpha-1)p(\cosh qL-1)q^{-2} - (\alpha+1)(\sinh qL)q^{-1} - \varepsilon/2\}}{\{(1+h_e\alpha^{-1})(\sinh qL)pq^{-1} + (1-h_e\alpha^{-1})\cosh qL\}}\ \tilde{u}_2(p) \qquad (61)$$

3. The transfer-function matrix and inverse Nyquist loci

Choosing $\tilde{q}_1(h,p)$ and $\tilde{q}_2(h,p)$ as the system outputs and $\tilde{u}_1(p)$ and $\tilde{u}_2(p)$ as the inputs then, from equation (56), (57), (58), which contain only diagonal coefficient matrices, and it is clear that the system dynamics may be described by

$$\tilde{\underline{q}}(h,p) = \underline{G}(h,p)\ \tilde{\underline{u}}(p) \qquad (62)$$

where $\underline{G}(h,p)$ is a diagonal transfer-function matrix (T.F.M), i.e.

$$\underline{G}(h,p) = \begin{pmatrix} g_1(h,p) & , & 0 \\ 0 & , & g_2(h,p) \end{pmatrix} \qquad (63)$$

Alternatively and for control design, purposes, more conveniently, the dynamics may be defined in terms of the inverse T.F.M. $\underline{G}^*(h,p)$ as follows

$$\tilde{\underline{u}}(p) = \underline{G}^*(h,p)\ \underline{q}(h,p) \qquad (64)$$

where

$$\underline{G}^{*}(h,p) \triangleq \underline{G}^{-1}(h,p) = \begin{bmatrix} g_1^{*}(h,p) & , & 0 \\ 0 & , & g_2^{*}(h,p) \end{bmatrix} \qquad (65)$$

Because of the diagonal structure, the relationship between the direct and inverse T.F.M. elements are simply

$$g_1(h,p) = 1/g_1^{*}(h,p)$$

and

$$g_2(h,p) = 1/g_2^{*}(h,p)$$

Confining attention to the accumulator and reboiler ends of the column by choosing h = 0, it therefore follows from equation (60) and (61) that

$$g_1^{*}(0,p) = \frac{\{(1-h_e\alpha^{-1})(\sinh qL)qp^{-1} + (1+h_e\alpha^{-1})\cosh qL\}}{\{(\alpha-1)(\cosh qL-1)p^{-1} - (1+\alpha)(\sinh qL)q^{-1} - \varepsilon/2\}} \qquad (66)$$

and

$$g_2^{*}(0,p) = \frac{\{(1+h_e\alpha^{-1})(\sinh qL)pq^{-1} + (1-h_e\alpha^{-1})\cosh qL\}}{\{(\alpha-1)p(\cosh qL-1)q^{-2} - (\alpha+1(\sinh qL)q^{-1} - \varepsilon/2\}} \qquad (67)$$

Fig. 6 shows the system's inverse Nyquist locus of $g_1^{*}(o,j\omega)$ computed from equation (66) for the normalised plant parameter values $\varepsilon = 0.75$, $(\alpha = 1.75)$, $L = 2.8$ and $T_a = T_b = 5.0$ whilst Fig. 7 shows the locus of the same element for a longer column having the parameters $\varepsilon = 1.0$, $(\alpha = 2.0)$, $L = 5.0$ and again, $T_a = T_b = 5.0$. Figs. 8 and 9 show the locus shapes traced out by $g_2^{*}(o,j\omega)$ for the shorter and longer columns respectively.

All four traces exhibit loops resembling those resulting from travelling waves encountered in heat exchanger analysis[8,9]. Like the case of the liquid/liquid counterflow heat exchanger. The basic locus shape, disregarding the superimposed loops, is however, similar to that of a first-order lag $(a+bp)^{-1}$ i.e. a vertical straight-line in the case of Figs. 6,8 and 9 indicating that a simple lag-(or, for higher performance controller synthesis, a simple lag-delay), structure might provide a satisfactory process approximation as with simulated tray-type columns. Unfortunately however, the behaviour of $g_1(o,p)$ for the longer packed column (Fig. 7) does not accord with the behaviour of a first-order lag due to the encirclement of the origin by $g_1^{*}(o,j\omega)$ suggesting non-minimum phase behaviour in this case.

4. Discussion and Conclusions

A transfer-function matrix (T.F.M.) model has been derived for a symmetrical packed binary distillation column completely analytically with the result that the model parameters are all expressed as simple functions of the plant parameters, namely α, the initial slope of the linearised equilibrium curve, L, the normalised length of each of the two column sections and T the normalised time-constant of the terminating vessels (the accumulator and reboiler). The model is expressed in terms of normalised frequency p, and normalised distance h, from the top and bottom of the column. (Conversion of normalised to actual distance requires multiplication by V/k and normalised to actual time by H/k, where V is the molar vapour flow rate, k the evaporation constant p.u. length and H the molar capacitance of the column p.u. length for liquid or vapour).

The process T.F.M. is found to be completely diagonal at all frequencies if the selected output vector is

$$\underline{q}(h) = \left[y(h) - x'(h) \;,\; y(h) + x'(h)\right]^T$$

and the selected input vector is

$$\underline{u} = (G/V)\left[(v+\ell),\; (v-\ell)\right]^T$$

where y and x' are the vapour and liquid composition changes in rectifier and stripper respectively, v and ℓ are changes in the applied vapour and reflux rates and G is the normalised static composition gradient through the column. In other words,

$$\tilde{\underline{u}}(p) = \underline{G}^*(h,p)\; \tilde{\underline{q}}(h,p)$$

where inverse T.F.M. $\underline{G}^*$ takes the diagonal form:

$$\underline{G}^*(h,p) = \begin{bmatrix} g_1^*(h,p) & , & 0 \\ 0 & , & g_2^*(h,p) \end{bmatrix}$$

This is an important result for the achievement of noninteracting control and is in broad accordance with empirical findings reported by some earlier researchers [1,11,12] and earlier analytical [10] work by the present author on tray distillation columns. Here the relationship is rendered precisely for the symmetrical column and it is reasonable

to suppose that small deviations from symmetrical operation would introduce small, possibly unequal, off-diagonal terms in the T.F.M. without serious detriment to controller performance. In situations of gross asymmetry between rectifier and stripping sections, the column would probably be better analysed as a single-stage process: a much easier task than the two-stage analysis reported here.

The derivation of $\underline{G}^*(h,p)$ has been greatly aided by the use of the "inverted U-tube" representation of the column particularly for terminal composition changes which are, of course, of prime importance.

The inverse T.F.M. elements $g_1^*(h,p)$ and $g_2^*(h,p)$ are found to involve hyperbolic functions of complex frequency p that produce loops in the inverse Nyquist loci resulting from travelling-wave phenomena in the column. From the loci computed it would appear that the composition "tilt" gain $g_1(o,o)$ can change sign, being positive for longer columns (in accordance with previous experience of tray-type columns) but becoming negative for shorter columns. Unlike tray-columns, the gain $g_1(o,p)$ at high frequency is negative for all packed columns suggesting non-minimum phase characteristics in the behaviour of the taller plants.

These preliminary deductions made from the derived parametric model suggest the need for caution in applying approximate low-order transfer-functions to column dynamics for the purpose of control system design. A fuller investigation of the implications for column behaviour to be drawn from the derived model is presented in a companion paper[3].

5. References

1. Shinskey, F.G., "Process control systems", 1967 (New York:McGraw Hill).
2. Stainthorp, F.P. and Searson, H.M., Trans. I.Chem.E., 1973, 51,42.
3. Edwards, J.B. and Guilandoust M., "An analytically-derived, parametric transfer-function model for ideal, packed, binary distillation columns, Part II: Behavioural predictions", Trans. I.Chem.E.
4. Edwards, J.B. and Tabrizi, M.H.N., "An analytically-derived, parametric transfer-function model for ideal, tray-type, binary distillation columns, Part I: Model development", ibid.
5. Edwards, J.B. and Tabrizi, M.H.N., "An analytically-derived, parametric transfer-function model for ideal, tray-type, binary distillation columns, Part II: Behavioural predictions", ibid.
6. Owens D.H., 'First and second-order-like structures in linear multi-variable control systems design', Proc. I.E.E., 1975, 122, (9), pp. 935-941.

7. Owens, D.H.: 'Feedback and Multivariable Systems', I.E.E. Control Engineering Series 7, Peter Peregrinus, 1978, 320pp.

8. Edwards, J.B., and Owens, D.H., 'First-order type models for multivariable process control', Proc. I.E.E., 1977, 124, (11), pp. 1083-1088.

9. Friedly, J.C., 'Asymptotic approximations to plug-flow process dynamics', A.I.Ch.E., June 1967.

10. Edwards, J.B., and JASSIM H.J., 'An analytical study of the dynamics of binary distillation columns', Trans. Inst. Chem. Eng., 1977, 55, pp. 17-29.

11. Rosenbrock, H.H. and Storey, C., 'Computational techniques for Chemical Engineers', 1966, (London: Pergammon Press).

12. McMorran, P.D., 'Application of the inverse Nyquist method to a distillation column model', Proc. of 4th U.K.A.C. Control Convention, 1971, p. 122.

6. Acknowledgements

Advice from Dr. D.H. Owens on the possibility of formulating and synthesising general lag-delay structures for distributed multivariable processes is gratefully acknowledged. This objective has provided a major motivation for the work here reported.

7. List of symbols

α	-	initial slope of equilibrium curve approximation
β	-	relative volatility of mixture
c	-	ratio of rectifier vapour-/stripper liquid capacitance
D	-	molar distillate rate
F_ℓ, F_v	-	molar feed rates of liquid and vapour = F, where equal
G	-	normalised spatial composition gradient in steady state
$\underline{G}$	-	transfer function matrix (T.F.M.)
$\underline{G}^*$	-	inverse T.F.M.
$\underline{G}_A^*$	-	inverse T.F.M. of multivariable first-order lag approximation
g_1^*, g_2^*	-	diagonal elements of $\underline{G}^*$
g_{A1}^*, g_{A2}^*	-	diagonal elements of $\underline{G}_A^*$
$H_\ell, H_\ell' (=H_2)$	-	liquid capacitances p.u. length of rectifier and stripper
$H_v (=H_1), H_v'$	-	vapour capacitances p.u. length of rectifier and stripper
h'	-	distance along column (measured from feed point in Section 1 and from ends from Section 2.2)
$\delta h'$	-	length of small cell of column
h	-	normalised distance (h' k/V)
$h_a(p), h_b(p)$	-	transfer functions of accumulator and reboiler {$=h_e(p)$ where identical}
$\underline{I}$	-	unit diagonal 2x2 matrix
k_r, k_s	-	rectifier and stripper coefficients of cross-flow (evaporation) p.u. length (=k where identical)
$\underline{K}$	-	controller gain matrix
k_1, k_2	-	diagonal elements of $\underline{K}$
L_1', L_2'	-	lengths of entire rectifier and stripper (=L' where identical)
L	-	normalised value of L'
$L_r (=L), L_s, \ell$	-	molar flows of liquid in rectifier and stripper and small changes therein
n	-	cell number
p	-	Laplace variable for transforms w.r.t. τ

q	-	$(p^2+2p)^{0.5}$
$\underline{q}$	-	vector of difference and total of vapour and liquid composition changes
$\underline{r}$	-	vector of associated equilibrium values
s	-	Laplace variable for transforms w.r.t. h
t	-	time
τ	-	normalised time ($=tk/H_2$)
T_a, T_b	-	normalised time-constants of accumulator and reboiler ($=T$ where identical)
$\underline{u}$	-	vector of total and difference vapour and reflux rate changes
$V_r(=V), V_s, v$	-	molar flows of vapour in rectifier and stripper and small changes therein
W	-	molar flow rate of bottom product
X, X'	-	liquid compositions (mol fractions) in rectifier and stripper
x, x'	-	small changes in X and X'
X_e'	-	Y_e'/α
x_e'	-	small changes in X_e'
Y, Y'	-	vapour compositions in rectifier and stripper
y, y'	-	small changes in Y and Y'
Y_e	-	X_e/α
y_e	-	small changes in Y_e
Z	-	feed liquid composition
z	-	feed vapour composition
$\approx$	-	superscript denoting Laplace transforms w.r.t. h and τ
$\sim$	-	" " " " " τ only

Appendix 1

Calculation of steady-state composition profiles

For the symmetrical column, this involves the solution of p.d.e.'s (16) subject to the special case boundary conditions (21), (23), (29) and (30), ignoring all time derivatives.

Hence, setting $Q(h) = 1-Y(h)$ ...(A1.1)

and $Q_e(h) = 1-Y_e(h)$ ...(A1.2)

we have to solve

$$\left.\begin{aligned} dQ/dh &= Q_e-Q \\ dQ_e/dh &= Q_e-Q \end{aligned}\right\}, \quad 0 \leq h \leq L$$

$$\left.\begin{aligned} dX'/dh &= X'-X_e' \\ dX_e'/dh &= X'-X_e' \end{aligned}\right\}, \quad -L \leq h \leq 0 \qquad \ldots(A1.3)$$

, if $L_1 = L_2 = L$

subject to $Q(L) = \alpha Q_e(L)$

$X'(-L) = \alpha X_e'(-L)$ ...(A1.4)

and $X_e'(0) + Q(0) = 2/(\alpha+1)$

$Q_e(0) + X'(0) = 2/(\alpha+1)$ ...(A1.5)

It follows immediately from the two pairs of d.e.'s that

$$dQ/dh = dQ_e/dh \triangleq -G = \text{constant}$$

and $dX'/dh = dX_e'/dh \triangleq G' = \text{constant}$ ...(A1.6)

Now from the second pair of boundary conditions (A1.5) it is clear that

$$Q(0) - Q_e(0) = X'(0) - X_e'(0) \qquad \ldots(A1.7)$$

so that, from (A1.3), (A1.6) and (A1.7) it follows that

$$G = G' \qquad \ldots(A1.8)$$

so yielding equation (31) in the main text.

From the system symmetry it is clear that

$$Q(h) = X'(-h) \quad \text{and} \quad Q_e(h) = X_e'(-h) \qquad \ldots(A1.9)$$

so yielding equation (36) in the main text.

Calculation of G

From (A1.3) and (A1.6)

$$G = Q - Q_e = Q(0) - Q_e(0) \qquad \ldots(A1.10)$$

and from (A1.5) and (A1.9) we get

$$Q_e(0) + Q(0) = 2/(\alpha+1) \qquad \ldots(A1.11)$$

so that, eliminating $Q_e(0)$ between (A1.10) and (A1.11)

$$2Q(0) = G + 2/(\alpha+1) \qquad \ldots(A1.12)$$

or, eliminating $Q(0)$, we get

$$2Q_e(0) = -G + 2/(\alpha+1) \qquad \ldots(A1.13)$$

But $Q(L) = Q(0) - GL$

and $Q_e(L) = Q_e(0) - GL$

and from the terminal boundary conditions, (A1.4), we therefore obtain

$$Q(0) - GL = \alpha Q_e(0) - \alpha GL$$

or $$G\varepsilon L = \alpha Q_e(0) - Q(0)$$

so that, eliminating $Q_e(0)$ and $Q(0)$ using (A1.12) and (A1.13) produces

$$G = 2\varepsilon/\{(\alpha+1)(2\varepsilon L + \alpha + 1)\} \qquad \ldots(A1.14)$$

as stated in the main text.

Calculation of $Q(0)$ and $Q_e(0)$ etc

Substituting for G in the foregoing expressions for $Q(0)$ and $Q_e(0)$, i.e. equations (A1.12) and (A1.13) respectively yields

$$Q(0) = 2(\alpha+\varepsilon L)/\{(\alpha+1)(2\varepsilon L+\alpha+1)\} \qquad \ldots(A1.15)$$

and $$Q_e(0) = 2(1+\varepsilon L)/\{(\alpha+1)(2\varepsilon L+\alpha+1)\} \qquad \ldots(A1.16)$$

from which by subtracting the composition change GL, we deduce

$$Q(L) = 2\alpha/\{(\alpha+1)(2\varepsilon L+\alpha+1)\} \qquad \ldots(A1.17)$$

and $$Q_e(L) = 2/\{(\alpha+1)(2\varepsilon L+\alpha+1)\} \qquad \ldots(A1.18)$$

{The results cross-check since subtracting either (A1.18) from (A1.17) or (A1.16) from (A1.15) produces the result

$$Q - Q_e \text{ (= constant)} = 2\varepsilon/\{(\alpha+1)(2\varepsilon L+\alpha+1)\} = G \qquad \ldots(A1.19)$$

as expected from (A1.10).}

Equations (A1.14) to (A1.19) form the basis from which the linear composition profiles of Fig.4 are constructed.

Fig. 1 Illustrating the complete system

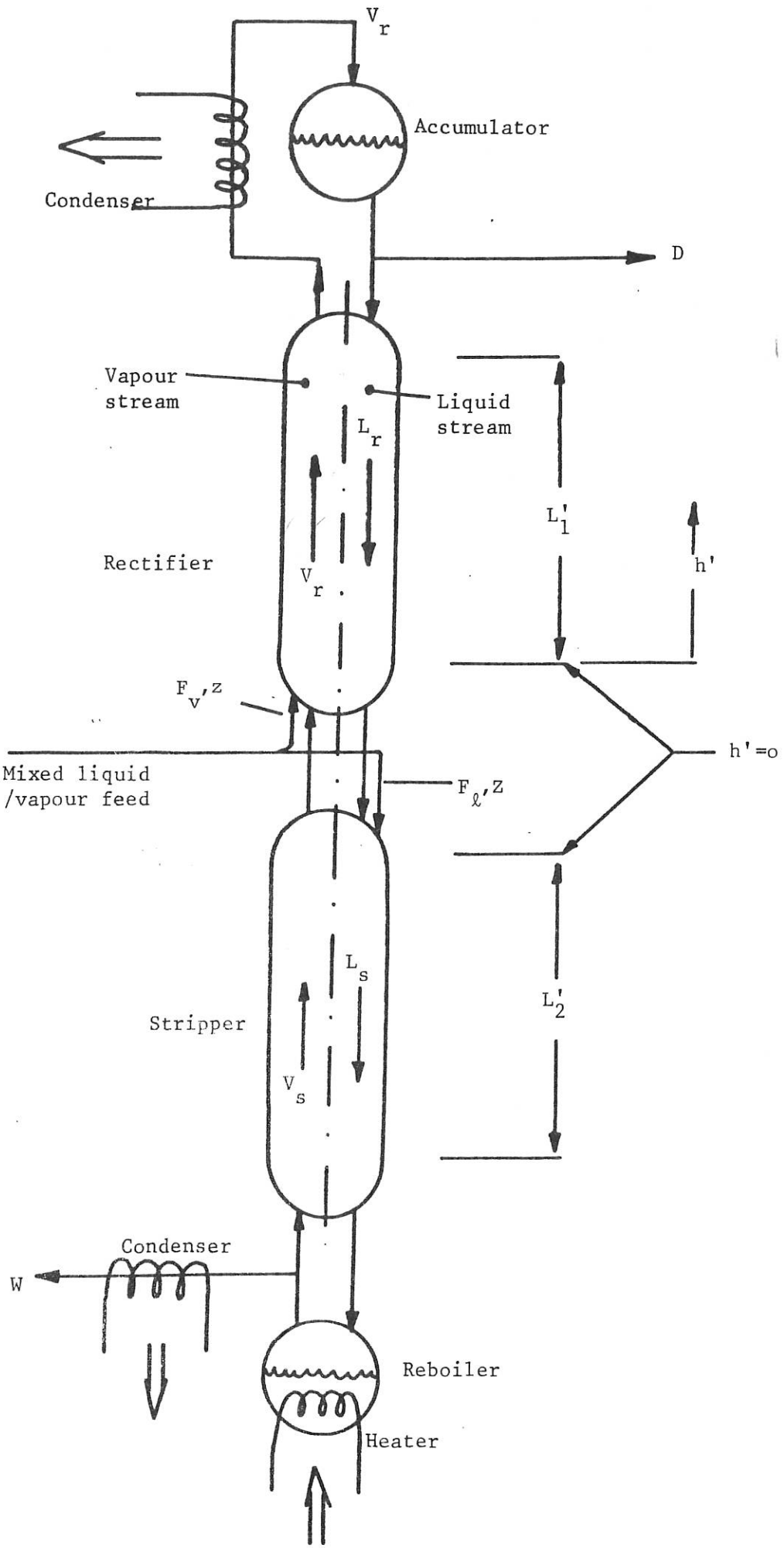

Fig. 2 General Rectifier Section

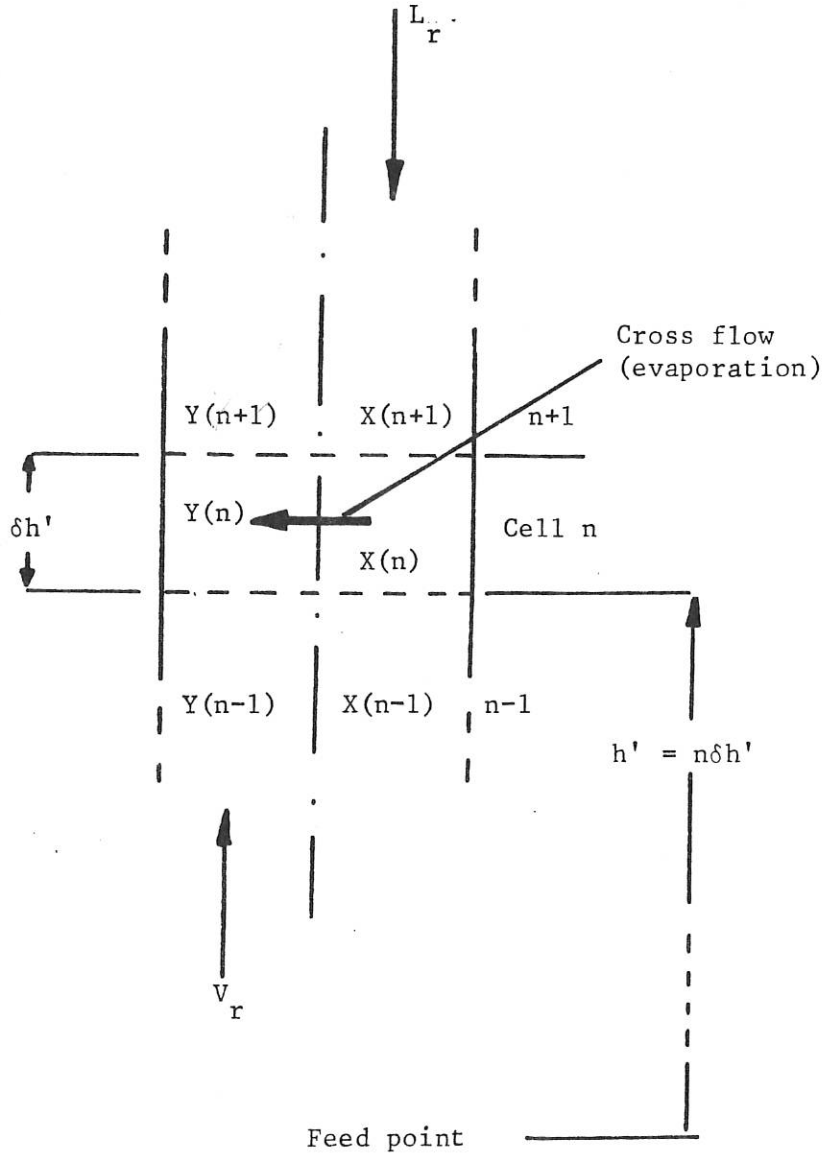

Fig. 3 Vapour/liquid equilibrium curve and its piecewise linear approximation

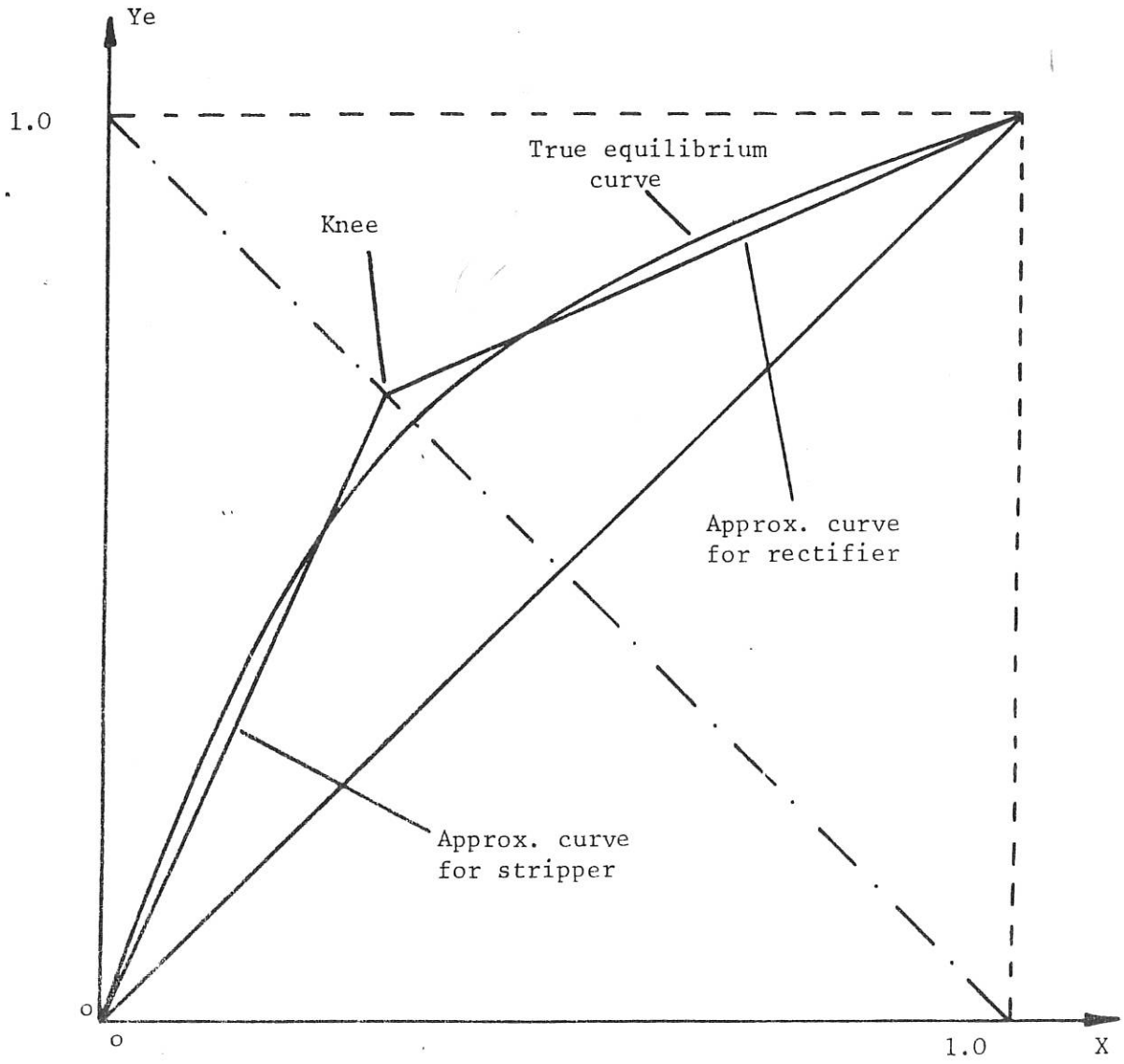

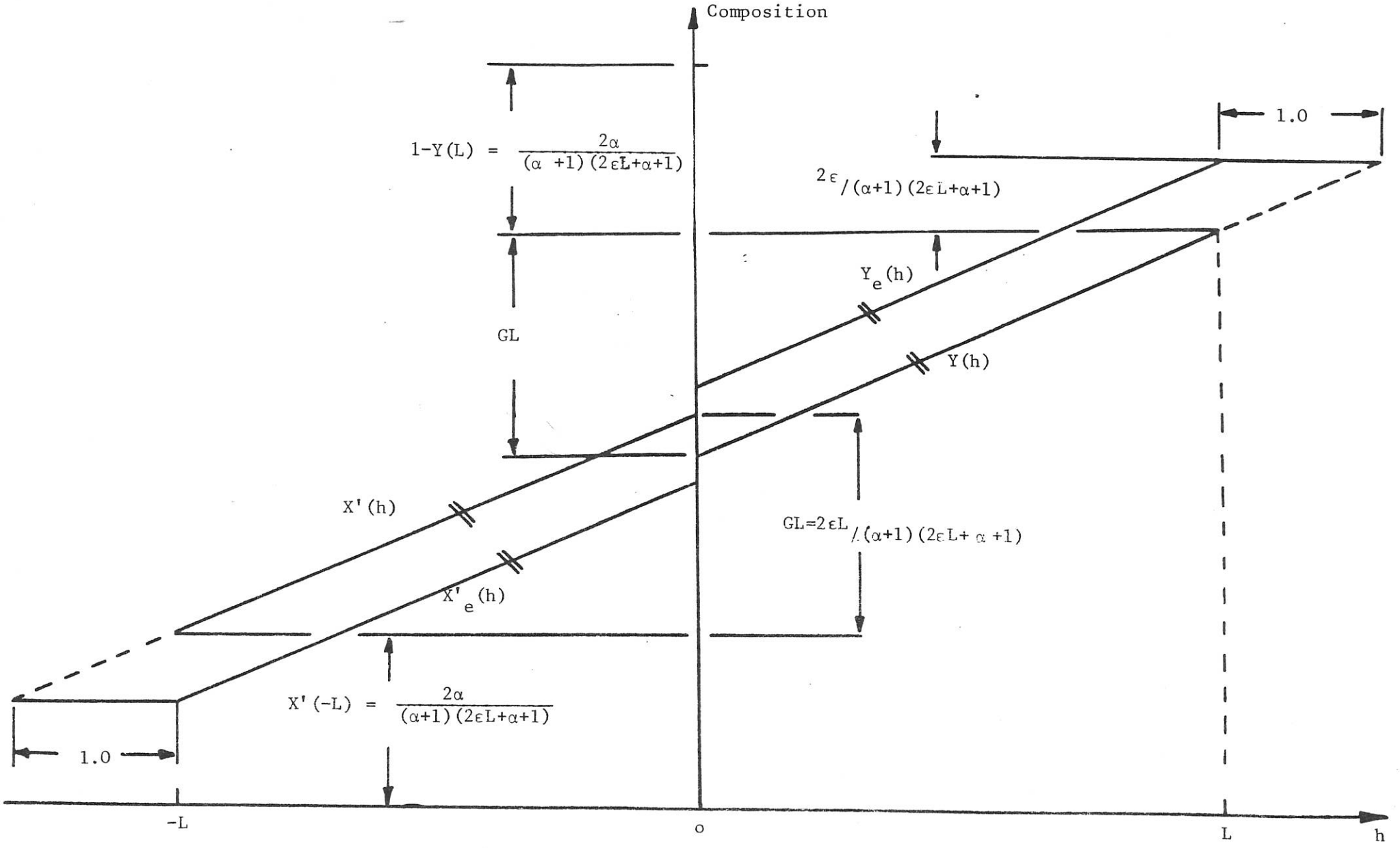

Fig. 4 Steady-state composition profiles

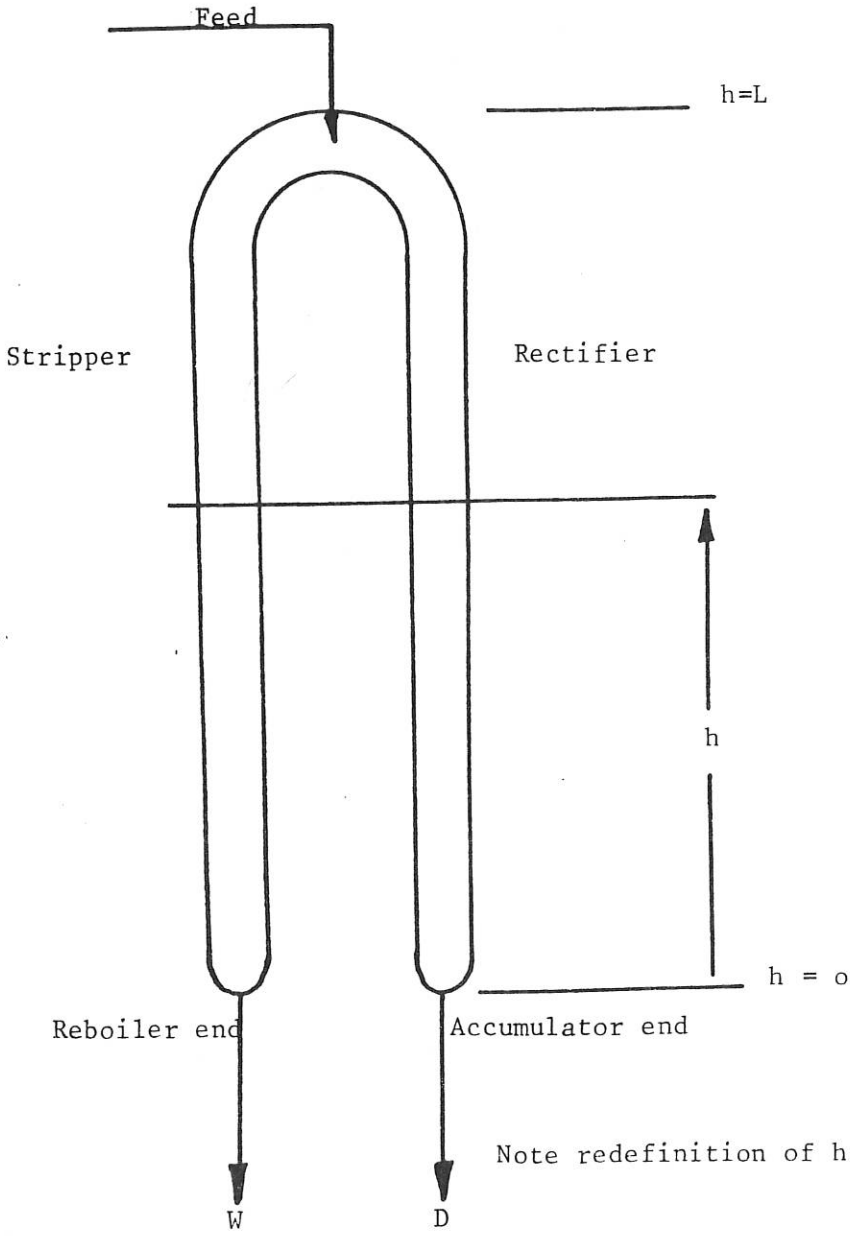

Fig. 5 Inverted U-tube model

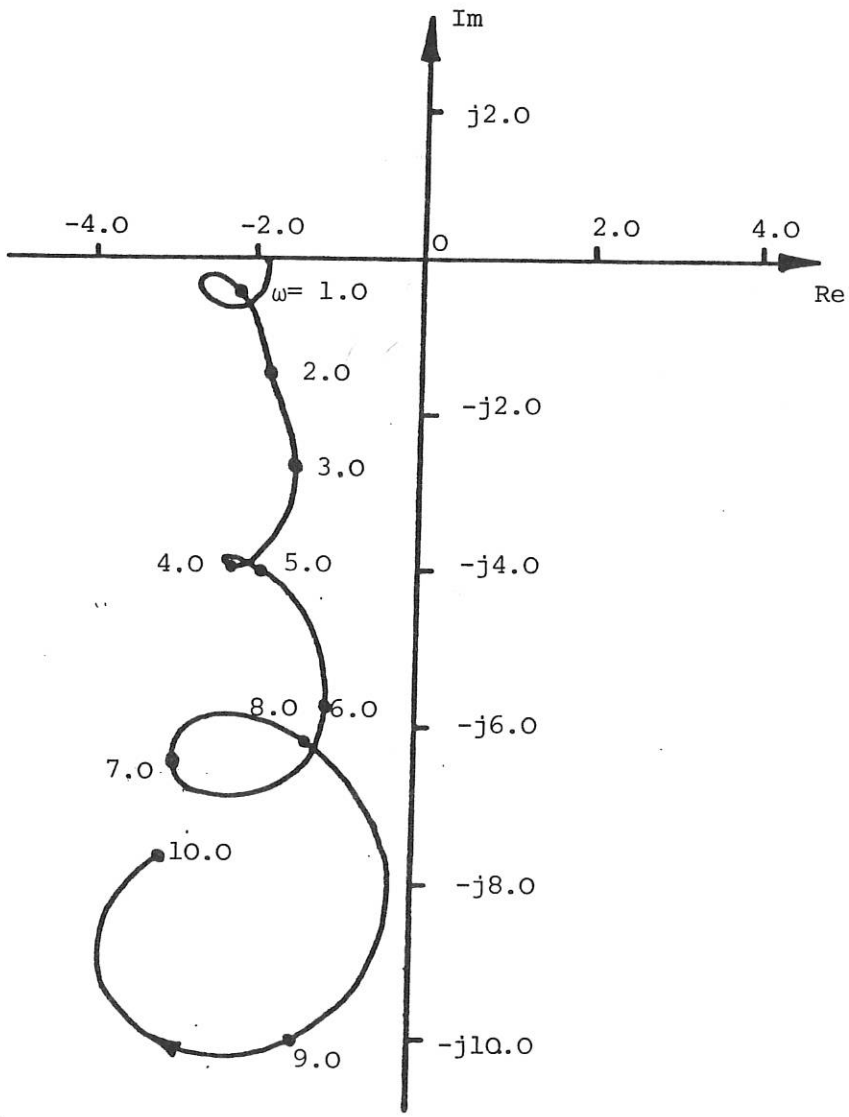

Fig. 6. Inverse Nyquist locus of $g_1^*(o,j\omega)$ for shorter column

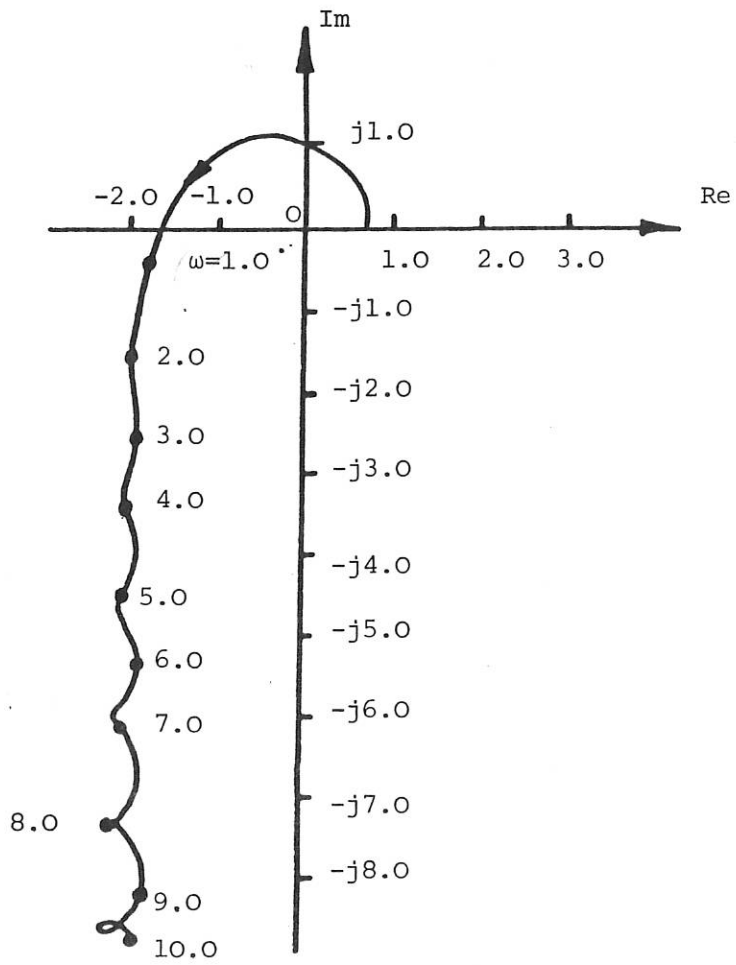

Fig. 7 Inverse Nyquist locus of $g_1^*(o,j\omega)$ for longer column

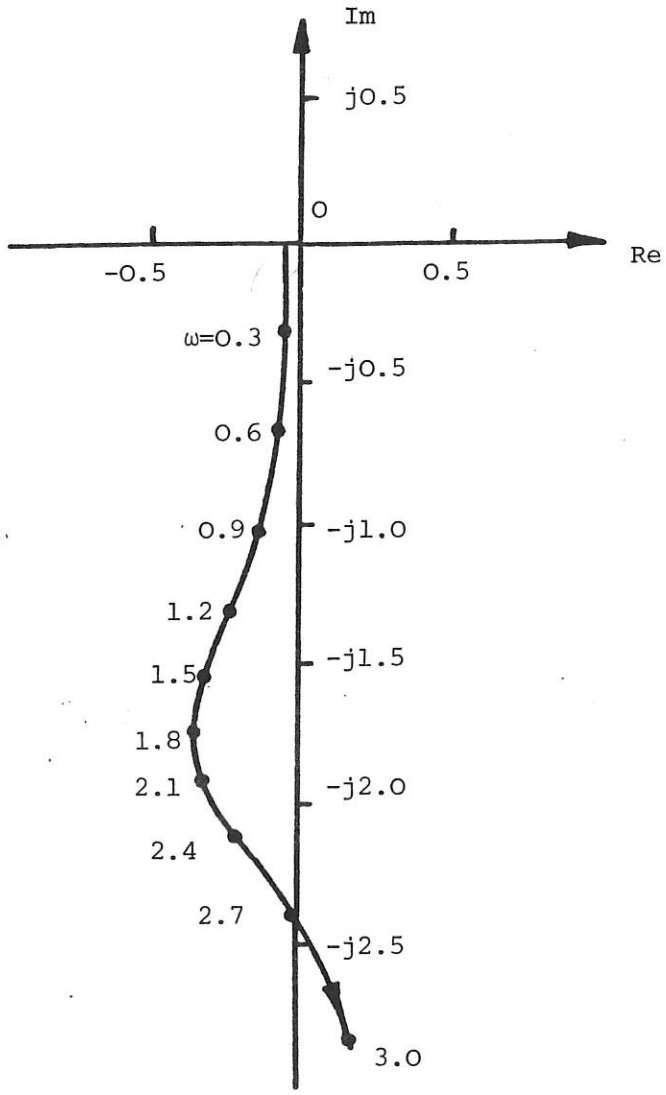

Fig. 8 Inverse Nyquist locus of $g_2^*(o,j\omega)$ for shorter column